9.9 Verification of RUC Surface Forecasts at Major U.S. Airport Hubs

Barry E. Schwartz* and Stanley G. Benjamin
NOAA Research–Forecast Systems Laboratory
Boulder, Colorado

1. INTRODUCTION

The Rapid Update Cycle (RUC) model running operationally at the National Centers for Environmental Prediction (NCEP) provides high-frequency mesoscale analyses and short-range numerical weather prediction guidance for aviation, severe weather, and general weather forecasting. In spring of 2002, a new 20-km version of the RUC (henceforth referred to as the RUC20) will replace the operational 40-km version (RUC40) running at NCEP. In addition to higher horizontal resolution, the new version of the RUC features a cloud analysis scheme and various other enhancements that include improvements to cloud microphysics, land-surface, and convective parameterizations. In addition, the RUC20 contains more detailed specifications of topography, land-use and soil-type fields. These changes have led to improvements in surface temperature, humidity, wind, and precipitation forecasts in the sample of forecasts examined by Schwartz and Benjamin (2001). See Benjamin et al. (2002) for a more complete description of of the RUC20.

Here, surface METAR observations are used to verify surface RUC40 and RUC20 3-h forecasts of 2 m temperature and 10 m wind speed at 27 major U.S. airport hubs. As of this writing, the sample of representative forecasts that are appropriate for verification (January 2002) is limited because of ongoing modifications to the RUC20 code in preparation for implementation. At the conference we plan to present a larger sample of statistics. See Smith and Benjamin (2002, this volume) for an interesting case study and statistical comparison of RUC40 and RUC20 visibility forecasts.

After the verification results, we briefly discuss the difficulty of using numerical models to forecast surface weather parameters and systematic problems related to the RUC20 that affect surface weather forecasts. All of the results here must be interpreted with the understanding that the RUC surface forecasts are a product of 1) the RUC analysis (especially its use of surface data), 2) the RUC forecast model (including its land-use specifications, surface-layer, boundary-layer, and land-surface physics), and 3) the RUC post-processing (including reduction to 2-m temperature and 10-m winds from a RUC computational level at 5 m above the ground via similarity theory, and use of a different grid elevation field (TOPOMINI) designed to more closely match METAR elevations than the model grid elevation). The precision of the RUC land-use specification compared to the actual METAR observation siting is also important.

2. VERIFICATION METHOD/RESULTS

Verification of 3-h surface RUC forecasts was performed by bilinearly interpolating temperature, humidity, winds, ceiling, and visibility forecasts to ~1500 METAR locations in the U.S., Canada, and Mexico. For this study, temperature and wind speed verification results are presented for the list of U.S. airport hubs (Table 1) for observations taken at 0000, 0300,....2100 UTC. Results for each location were averaged over the month of January 2002 for each 3-h observation time.

Tables 2 and 3 show the verification results for each location and time of day for temperature and wind speed, respectively. The bias value is the mean forecast-minus-observed (F- O) and the improvement over persistence (%PER) compares the average root mean square (rms) forecast error (f) against the rms persistence forecast error (p), defined as (p-f)/max(p,f). Here the persistence forecast is simply the temperature (or wind speed) observation 3 h previous to the verification time.

Table 2 indicates that for most of the hubs, the RUC20 exhibits a cold bias for this verification sample. According to the %PER score, the RUC20 forecast is poorer than persistence at night (0600 and 0900 UTC) at many locations, which is not unexpected since persistence is hard to beat during times of constant temperature. In general, the RUC20 verifies the best at inland locations and the worst along coastal areas. This is more evident when the results are examined at all ~1500 METAR locations (not shown). For example, hubs such as KORD (Chicago/O'Hare, Fig. 1) and KMCI (Kansas City, not shown) show considerably less bias for RUC20 and higher %PER than at KLGA (LaGuardia, New York, NY, Fig 2) and KLAX (Los Angeles, CA, Fig. 4).

Table 3 shows the results for wind speed. Comparison of

Table 2 and Table 3 indicates that RUC forecasts more consistently improve upon persistence for wind speed than for temperature. However, as seen for temperature, it is still difficult to beat persistence at night in many locations. As was the case for temperature, wind forecasts are generally more accurate at inland locations than along coastal areas.

Table 4 compares 2-m temperature 3-h forecast verification from the operational RUC40 and the RUC20. In this table, the column values contain the RUC20 minus the RUC40 value for the bias and %PER. Although for this sample of locations the results are mixed, the RUC20 is clearly much improved over the RUC40 during the daytime at most locations (1200– 2100 UTC).

3. DISCUSSION

As discussed briefly in the introduction, there are various factors that affect the accuracy of surface sensible weather forecasts from all numerical weather prediction (NWP) models. In the RUC, as in any NWP model, constant use fields such as topography, land use, and soil types strongly affect the surface forecast fields. Although these fields are now available to the RUC20 at higher resolution, these fields are still not sufficient to fully resolve mesoscale variations in surface weather due to phenomena such as urban heat island effects, local drainage, and land-sea breezes, or peculiar or "unrepresentative" observational sitings.

An excellent example of mesoscale variability in local observations routinely occurs in the New York City area. Notice the large difference in the performance of the RUC20 temperature forecasts at KLGA (Fig. 2) and KJFK (Fig. 3) which are separated by only a few kilometers. The average January 2002 temperature computed from the plethora of observations in the New York City area (not shown) indicates that KLGA is the warmest site at almost all times of the day; it is even warmer than the observation taken at Central Park. Assuming that KLGA is not erroneous, it is likely that the observational site is prone to urban heat island effects. NWP models cannot resolve such effects until they reach horizontal resolution of 1 or 2 km. Tradi-tionally, techniques such as Model Output Statistics (MOS; Glahn and Lowry, 1972) are often more successful at resolving such variability. Unfortunately, the development of an accurate set of MOS forecast equations requires a "stable" (nonchanging) sample of NWP model output, usually considered to be a minimum of two years of data for all four seasons.

An example of how the resolution of the model topo-graphy affects the 3-h RUC20 surface temperature forecast is shown in Figure 5. This is a scatterplot of the elevation difference (TOPOMINI elevation [see section 1] – METAR elevation) against the 3-h average forecast error at all ~1500 METAR sites for January 2002. The largest cool (warm) biases occur at sites that have a large positive (negative) elevation difference (most of which are in mountainous regions). Reduction of 2-m tempera-tures from the RUC to the TOPOMINI elevation field instead of the original model elevation reduces the problems shown in Fig. 5, but clearly does not eliminate it.

The verification results for KLAX (Fig. 4) and other locations along both the West and East coast (not shown) indicate that the RUC20 has more difficulty forecasting accurate surface conditions at coastal locations because the RUC land-use field does not adequately resolve coastlines. This can result in a water surface-type field at the model grid points closest to the station location (on land). If the RUC treats a grid point as if it were water near a METAR, the exchange of heat, moisture, and momentum from the surface will likely be inaccurate for the METAR location. Verification of offshore buoys along both coasts (not shown) shows smaller errors, which supports the hypothesis that inadequate resolution in the land-use field, even at 20 km, contributes to RUC surface forecast errors in coastal areas.

Since it is not yet possible to develop MOS equations to improve the forecast of surface weather parameters from many NWP models, field forecasters have no choice but to use surface forecasts *directly* from NWP models. We have shown that for many places, the RUC20 provides useful short term surface forecasts. Table 4 indicates that the RUC20 will provide improved guidance over the RUC40 at many locations particularly during the day. The improvements over the RUC40 from RUC20 wind speed forecasts are similar (not shown). Nevertheless, we believe that further improvements can be made to the RUC post processing which is used to derive surface weather forecasts. Studies such as this provide clues as to how this might be done. For example, it might be possible to routinely compute recent individual station biases and apply them to adjust current NWP forecasts in a "poor man's MOS" fashion, or to separately postprocess the surface forecasts by using the actual station elevation when interpolating from the lowest model level to the METAR locations.

4. REFERENCES

Benjamin, S.G., J.M. Brown, D. Devenyi, G.A. Grell, D. Kim, T.L. Smith, T.G. Smirnova, B.E. Schwartz, S. Weygandt, and G.S. Manikin: 2002: The 20km Rapid Update Cycle–Overview and implications for aviation applications. This volume.

Glahn, H.R., and D.A. Lowry, 1972: The use of Model Output Statistics (MOS) in objective weather forecasting. *J. Appl Meteor*., **11**, 1203–1211.

Schwartz, B.E., and S.G. Benjamin, 2001: Verification of 20-km RUC surface and precipitation forecasts. *Preprints, 14th Conf. on Numerical Weather Prediction, Fort Lauderdale, FL, Amer. Meteor. Soc.,*138--141.

Smith, T.L., S.G. benjamin, and J.M. Brown, 2002: Visibility forecasts from the RUC20. This volume.

(1)

(2)

(3)

(4)

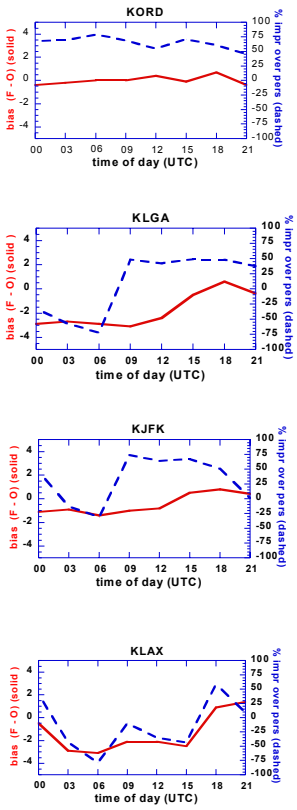

Figs. 1–4. 3-h RUC20 surface temperature forecast bias (F-O) and %PER for KORD, KLGA, KJFK, and KLAX for January 2002.

Table 1. U.S. Airport Hubs and Identifiers.

ID	Airport	ID	Airport	ID	Airport
KATL	Atlanta, GA	KIAD	Washington, DC	KORD	Chicago, IL
KBNA	Nashville, TN	KIAH	Houston, TX	KORL	Orlando,FL
KBOS	Boston, MA	KJFK	New York (JFK), NY	KPHL	Philadelphia, PA
KCLT	Charlotte, NC	KLAX	Los Angeles, CA	KPHX	Phoenix, AZ
KCVG	Cincinnati, OH	KLGA	New York, NY	KPIT	Pittsburgh, PA
KDCA	Washington, DC	KMCI	Kansas City, MO	KSDF	Louisville, KY
KDEN	Denver, CO	KMEM	Memphis, TN	KSEA	Seattle, WA
KDTW	Detroit, MI	KMIA	Miami, FL	KSFO	San Francisco, CA
KDFW	Dal-Ft Worth, TX	KMSP	Minneapolis, MN	KSTL	St Louis, MO

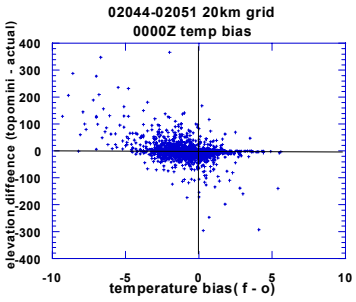

Fig. 5. 3-h RUC20 temperature forecast bias (F-O) versus elevation difference (TOPOMINI- METAR) for ~1500 stations for 13–20 February 2002.

Table 2. Bias (F-O) and percent improvement over persistence (%PER) for 3-h RUC temperature forecasts for January 2002.

HUB	00 UTC		03 UTC		06 UTC		09 UTC		12 UTC		15 UTC		18 UTC		21 UTC	
	bias	%	bias	%	bias	%	bias	%	bias	%	bias	%	bias	%	bias	%
KATL	-2.6	14	-2.0	19	-1.8	-15	-1.7	38	-1.2	65	-0.5	83	-0.8	67	-1.4	34
KBNA	-2.1	11	-1.9	12	-1.0	17	-1.2	67	-0.4	65	-1.3	59	0.1	77	-1.4	25
KBOS	-0.9	28	-0.8	-25	0.3	71	0.8	77	-0.1	80	-1.1	57	-1.2	54	-1.7	-4
KCLT	-1.6	57	-0.7	49	-0.7	25	-0.5	49	-0.1	71	-1.2	75	-0.6	74	-1.4	19
KCVG	-1.4	67	-0.5	69	0.3	73	-0.7	75	-1.2	70	-2.0	61	0.0	62	-0.2	51
KDCA	-1.9	28	-2.7	-51	-2.8	-47	-2.4	58	-2.7	65	-2.0	65	-0.2	75	-0.6	48
KDEN	0.5	43	0.5	76	-1.8	-7	-3.2	45	-2.4	60	-5.0	-33	0.1	67	1.3	57
KDFW	-0.5	52	-0.1	57	-0.5	71	-1.0	70	-1.2	64	-2.3	8	0.5	70	-0.3	64
KDTW	-0.8	40	0.3	34	0.1	20	0.5	62	0.0	61	-0.6	76	1.2	48	-0.5	47
KIAD	-1.0	66	-1.9	-10	-1.2	-2	-0.3	79	-0.4	71	-0.6	71	-0.1	72	-1.4	7
KIAH	-0.8	61	0.0	76	0.3	75	0.5	77	-0.5	0	-2.2	43	-0.4	86	-0.7	51
KJFK	-1.1	46	-0.9	-13	-1.4	-31	-1.0	74	-0.8	64	0.5	67	0.8	51	0.4	1
KLAX	-0.5	41	-2.9	-43	-3.1	-79	-2.1	-10	-2.1	-35	-2.5	-43	0.9	59	1.4	9
KLGA	-2.9	-32	-2.7	-57	-2.9	-72	-3.1	48	-2.4	42	-0.5	49	0.6	48	-0.4	37
KMCI	0.4	63	0.4	51	-1.9	-29	-0.9	59	-0.9	28	-2.3	0	-0.4	83	-0.3	48
KMEM	-1.4	46	-1.5	1	-1.8	12	-1.5	53	-1.6	35	-1.9	49	-0.3	54	-1.4	23
KMIA	-0.2	61	-1.0	-34	-0.7	31	-1.0	68	-0.6	19	-1.1	69	-0.5	66	-0.8	-8
KMSP	-1.0	62	-0.6	13	-0.9	38	-0.6	78	-1.0	66	-1.1	42	1.5	55	0.8	73
KORD	-0.4	68	-0.2	69	0.0	79	0.0	69	0.4	55	-0.1	71	0.7	61	-0.4	45
KORL	-1.8	21	-1.8	10	-1.5	-3	-1.6	41	-1.9	3	1.2	64	-0.5	49	-0.9	23
KPHL	-2.9	-16	-1.3	33	-2.2	-51	-2.0	66	-3.1	28	-1.6	34	-0.1	74	-1.2	24
KPHX	-2.4	-62	-5.8	-34	-3.4	-8	-3.6	-24	-3.7	-21	-2.1	-17	-0.7	64	0.4	53
KPIT	-1.4	0	-0.8	-20	0.0	4	0.3	79	1.4	53	-0.1	65	0.1	63	-1.4	4
KSDF	-2.5	35	-2.2	42	-1.3	5	-2.1	45	-1.3	67	-2.0	56	0.1	69	-1.4	46
KSEA	-0.5	37	-1.1	46	-1.1	7	-1.8	25	-1.4	35	0.0	48	0.4	57	1.2	55
KSFO	-1.8	-56	-0.3	50	0.1	-45	-0.5	7	0.5	-7	0.5	13	-0.6	53	-1.8	-21
KSTL	-2.2	-29	-1.2	50	-1.7	-3	-1.9	34	-2.0	39	-1.7	53	0.0	71	-0.8	34

Table 3. Same as Table 2 except for wind speed forecasts

HUB	00 UTC		03 UTC		06 UTC		09 UTC		12 UTC		15 UTC		18 UTC		21 UTC	
	bias	%	bias	%	bias	%	bias	%	bias	%	bias	%	bias	%	bias	%
KATL	0.2	67	-0.2	61	-1.1	20	-0.6	59	-0.9	75	1.9	27	-0.9	69	0.3	-14
KBNA	0.5	78	0.9	28	0.7	38	0.9	36	1.0	73	-0.2	72	-0.3	70	-0.2	60
KBOS	-0.4	68	-0.7	77	1.1	84	0.5	62	1.1	67	-0.4	65	-0.3	79	-1.0	71
KCLT	0.8	49	-0.5	61	0.5	40	0.0	24	-0.1	65	-0.5	82	-1.0	67	0.0	83
KCVG	-1.3	42	-1.0	87	-0.2	46	-0.9	51	-1.1	54	-0.5	66	-1.5	29	-1.9	75
KDCA	-1.2	78	-0.2	74	-1.7	22	0.3	41	0.7	58	-2.5	70	-1.1	58	-1.3	52
KDEN	-0.5	63	0.3	55	0.3	6	-1.2	62	-1.9	64	-1.4	69	-1.1	55	-0.1	55
KDFW	-0.4	84	0.9	78	-0.5	67	-0.8	37	-0.3	84	0.1	64	-0.1	74	-0.4	64
KDTW	-1.6	82	0.3	81	0.1	42	0.5	58	0.2	83	0.1	93	1.1	42	-0.3	78
KIAH	-0.6	3	1.3	69	0.3	85	0.0	96	0.7	60	-0.4	89	-0.1	90	-0.2	28
KJFK	-1.6	59	-0.5	81	0.2	77	-0.8	74	0.4	79	-0.9	83	-1.9	41	0.0	78
KLAX	-2.0	55	0.2	69	0.7	31	0.8	54	3.3	-14	-2.0	-2	0.0	98	-2.0	15
KLGA	-1.7	52	-0.8	84	-0.6	62	-1.3	61	-1.0	69	-1.7	64	-1.0	74	-1.9	44
KMCI	0.6	81	0.7	63	-0.6	80	0.2	29	-0.6	82	0.6	76	0.8	61	0.1	64
KMEM	-0.2	63	0.3	74	-0.7	85	0.8	33	-0.1	81	-0.4	72	1.1	63	-0.9	67
KMIA	-0.1	54	0.2	51	0.4	13	1.1	38	0.6	45	-1.3	56	-2.0	54	-1.2	44
KMSP	-0.5	77	0.8	75	1.0	42	0.6	62	0.0	81	-0.1	85	1.6	-54	0.2	77
KOAK	-1.3	64	-0.2	79	0.3	51	-0.5	32	-1.1	76	-1.5	57	0.0	72	-1.3	61
KORD	0.2	79	0.8	89	0.8	65	0.9	21	0.0	78	-0.3	85	0.2	86	-0.2	76
KORL	0.1	64	0.7	74	0.2	33	0.0	93	0.1	62	-0.7	64	-0.4	12	-1.0	78
KPHL	-1.1	45	0.5	49	-0.1	47	0.5	53	-0.2	66	-1.2	78	-0.6	-4	-2.2	71
KPHX	-4.2	-9	1.8	33	1.4	40	0.3	43	1.0	33	0.1	69	-1.6	47	2.2	-5
KPIT	-0.3	68	0.0	78	0.7	38	0.1	32	-0.5	73	-0.9	53	0.5	82	-0.3	87
KSDF	-0.7	79	0.3	71	0.5	45	0.7	63	0.1	70	0.3	71	0.1	41	-0.9	32
KSEA	-1.1	53	-0.2	65	-2.4	5	-1.9	31	-0.8	13	-0.5	75	0.7	72	-1.6	57
KSFO	0.9	64	-0.3	81	1.2	39	0.6	76	0.1	57	0.7	69	0.3	61	0.8	69
KSTL	0.4	77	0.0	99	0.0	52	0.1	44	-0.6	80	-0.1	88	-0.5	59	-1.0	30

Table 4. RUC20 - RUC40 bias and %PER for January 2002.

HUB	00 UTC		03 UTC		06 UTC		09 UTC		12 UTC		15 UTC		18 UTC		21 UTC	
	bias	%	bias	%	bias	%	bias	%	bias	%	bias	%	bias	%	bias	%
KATL	0.5	-15	0.3	3	0.4	-44	0.4	-13	0.5	14	-2.0	11	-1.6	28	-0.7	-19
KBNA	0.4	-11	0.2	32	0.3	-48	-0.3	15	-0.2	90	-1.2	45	-1.0	21	-0.6	-7
KBOS	-1.3	48	-1.3	24	-1.6	93	-1.4	47	-1.8	52	-1.9	70	-1.1	22	-0.4	20
KCLT	0.5	-16	0.3	6	0.0	32	0.2	-4	0.2	4	-2.3	38	-1.4	24	-0.1	58
KCVG	0.5	-29	-0.1	15	0.4	-21	0.3	-3	0.2	-2	-1.2	31	-0.6	6	-0.2	53
KDEN	-0.9	20	0.4	7	0.1	-25	0.7	2	1.5	15	2.1	43	-1.1	14	0.9	72
KDFW	-0.9	15	0.1	5	-0.1	23	0.0	-10	-0.1	65	-0.2	-5	-0.4	-3	0.8	-20
KDTW	-0.4	3	-1.2	13	-0.7	-32	-0.2	35	0.0	20	-2.1	95	-0.9	9	-0.4	36
KIAD	0.5	5	-0.2	2	0.4	12	-1.0	30	-0.1	68	-1.0	7	-0.7	12	0.5	-6
KIAH	-0.2	6	0.0	28	0.3	-34	-0.2	13	-0.1	70	-1.1	32	-0.9	34	-0.8	25
KJFK	0.3	-5	0.2	3	0.1	-18	0.0	0	0.1	6	-1.6	52	-1.3	37	0.3	82
KLAX	-1.6	49	1.2	16	0.6	13	-0.3	8	-0.8	38	-0.2	50	-1.8	21	0.0	9
KLGA	0.4	-11	0.0	-2	-0.1	0	-0.2	6	-0.2	-56	-1.8	102	-1.9	40	0.2	-29
KMCI	-1.2	10	-0.2	-20	-0.1	-61	-0.1	-11	0.1	48	-0.9	68	-0.6	6	0.1	16
KMEM	0.4	-20	0.0	47	-0.1	-8	-0.2	10	-0.1	92	-1.5	28	-2.1	21	-1.1	75
KMIA	-0.4	7	0.2	23	0.2	-53	0.2	-16	0.4	75	-0.6	23	-1.2	13	0.1	-3
KMSP	-0.5	3	-0.7	113	-0.6	-52	0.1	-18	-0.2	17	-1.0	81	-0.4	-12	-0.1	6
KORD	-0.2	-6	-0.9	19	-0.6	41	0.5	-19	0.3	58	-1.4	44	-0.2	39	-0.4	12
KORL	0.3	0	-0.1	24	0.0	-52	0.4	-58	1.1	18	0.0	-2	-1.2	20	0.2	24
KPHL	0.9	-29	0.7	-1	0.7	-29	0.4	-11	0.6	12	-1.3	51	-1.2	16	0.5	55
KPHX	1.3	-35	2.2	-33	0.2	-3	0.5	-19	0.5	20	0.6	90	-0.6	11	0.7	-8
KPIT	-0.1	-6	-0.2	26	-0.3	-1	-0.4	21	-0.5	108	-1.6	87	-0.5	32	-0.6	16
KSDF	0.1	-5	-0.6	-4	-0.7	2	-0.7	13	-0.8	9	-2.1	47	-2.0	15	-0.4	-60
KSEA	0.3	16	0.0	-19	-0.2	-61	0.2	3	0.2	-31	-0.4	13	-1.0	9	-0.2	-3
KSFO	-0.1	17	0.7	-16	0.2	1	0.0	9	-0.1	50	0.4	10	-1.4	28	-0.5	32
KSTL	0.1	0	-0.3	24	-0.1	-60	0.3	-9	0.0	28	-1.5	75	-1.8	20	-0.5	54